

Evidence for excitation of polar motion by fortnightly ocean tides

Richard S. Gross, Kamal H. Hamdan and Dale H. Boggs

Jet Propulsion Laboratory, California Institute of Technology, Pasadena

Abstract. The second-degree zonal tide raising potential, which is responsible for tidal changes in the Earth's rotation rate and length-of-day, is symmetric about the polar axis and hence can excite the Earth's polar motion only through its action upon nonaxisymmetric features of the Earth such as the oceans. Ocean tidal excitation of polar motion in the diurnal and semidiurnal tidal bands has been previously detected and examined. Here, the detection of ocean tidal excitation of polar motion in the long-period tidal band, specifically at the Mf' (13.63-day) and Mf (13.66-day) tidal frequencies, is reported. Spectra of the SPACE94 polar motion excitation series exhibit peaks at the prograde and retrograde fortnightly tidal periods. After removing effects of atmospheric wind and pressure changes, an empirical model for the effect of the fortnightly ocean tides upon polar motion excitation is obtained by least-squares fitting periodic terms at the Mf and Mf' tidal frequencies to the residual polar motion excitation series. The resulting empirical model is then compared with the predictions of two hydrodynamic ocean tide models.

Introduction

The rotation of the solid Earth is not steady but exhibits changes in both: (1) angular speed, giving rise to changes in the length-of-day, and (2) the orientation of the rotation axis within the solid Earth, giving rise to the Earth's polar motion [e.g., *Eubanks, 1993*]. These changes in the rotation of the solid Earth are caused either by: (1) the action of surface forces applied at the solid Earth's interface with its overlying atmosphere and hydrosphere or underlying liquid core, or by (2) changes in the mass distribution of the solid Earth thereby changing its inertia tensor and hence rotation. The tide raising potential due to the gravitational attraction of the sun, Moon, and planets generates deformations of both the oceans, giving rise to the ocean tides, and the solid Earth, giving rise to the body tides. These tidally induced ocean currents and changes in the mass distribution of the oceans and solid Earth cause periodic changes in the Earth's rotation at the tidal frequencies.

Length-of-day changes caused by the deformation of the solid Earth due to the long-period body tides can be predicted from models of the solid Earth's elastic response to the tide raising potential [*Yoder et al., 1981*]. The ocean tides contribute to the tidally induced length-of-day changes [e.g., *Yoder et al., 1981*] and, because of the asymmetric distribution of the oceans on the surface of the Earth, they should also, in principle, excite polar motion. Diurnal and semidiurnal changes in polar motion have been recently detected and attributed to the effects of ocean tides [*Herring, 1993; Sovers et al., 1993; Herring and Dong, 1994; Watkins and Eanes, 1994*]. In this report, evidence is presented for the excitation of polar motion by the fortnightly ocean tides.

Fortnightly Polar Motion Excitation Signal

Polar Motion Excitation Series

The polar motion excitation data set used in this study is that derived from the SPACE94 Earth orientation series [*Gross, 1996*]. SPACE94 is a Kalman filter-based combination of independent Earth orientation measurements taken by the space-geodetic techniques of lunar laser ranging, satellite laser ranging, very long baseline interferometry, and global positioning system interferometry. The Kalman filter used in generating SPACE94 contains a model of the polar motion process and produces estimates of the Earth orientation excitation functions along with estimates of polar motion and universal time [*Morabito et al., 1988*]. The complex-valued polar motion excitation function $\chi(t)$ is the polar motion forcing function which, at frequencies far from the Free Core Nutation resonance, is related to polar motion $\mathbf{p}(t)$ through the expression [e.g., *Gross, 1992*]:

$$\mathbf{p}(t) + \frac{i}{\sigma_{cw}} \frac{d\mathbf{p}(t)}{dt} = \chi(t) \quad (1)$$

where $i = \sqrt{-1}$, $\mathbf{p}(t) = p_1(t) - i p_2(t)$, $\chi(t) = \chi_1(t) + i \chi_2(t)$, and σ_{cw} is the complex-valued frequency of the Chandler wobble. The subscripts 1 and 2 in the above definitions of $\mathbf{p}(t)$ and $\chi(t)$ denote their x and y components, respectively. The negative sign in the definition of $\mathbf{p}(t)$ is required due to the convention that the y component of polar motion, $p_2(t)$, is defined to be positive towards 90° W longitude, whereas the y component of polar motion excitation, $\chi_2(t)$, is defined to be positive towards 90° E longitude.

The SPACE94 polar motion excitation series consists of 6688 daily values of $\chi(t)$ spanning October 6, 1976 to January 27, 1995. A power spectrum of that portion of the SPACE94 polar motion excitation series spanning 1984–1994 is displayed in Figure 1a where the vertical dotted lines indicate frequencies in the weekly (9-day), fortnightly (14-day), and monthly (27-day) tidal bands. As can be seen, there appears to be relatively enhanced power in the prograde and retrograde fortnightly tidal bands, and perhaps the prograde weekly tidal band.

Atmospheric Angular Momentum Series

Significant sources of non-tidal excitation of polar motion, such as atmospheric wind and pressure fluctuations, should be removed from the SPACE94 excitation series prior to analyzing it for the presence of ocean tidal excitation. Of the atmospheric angular momentum (AAM) data sets currently available, the one with the greatest time span, and the only one that fully overlaps in time with the SPACE94 polar motion excitation series, is that determined from the global analyses produced under the global data assimilation system of the U.S. National Centers for Environmental Prediction (NCEP, formerly the U.S. National Meteorological Center).

Two different AAM pressure terms are available from NCEP, computed under two different assumptions for the response of the oceans to imposed atmospheric pressure changes: (1) the oceans are assumed to respond as an inverted barometer, in which case

Copyright 1996 by the American Geophysical Union.

Paper number 96GL01596
0094-8534/96/96GL-01596\$05.00

POLAR MOTION EXCITATION SPECTRA (1984–1994)

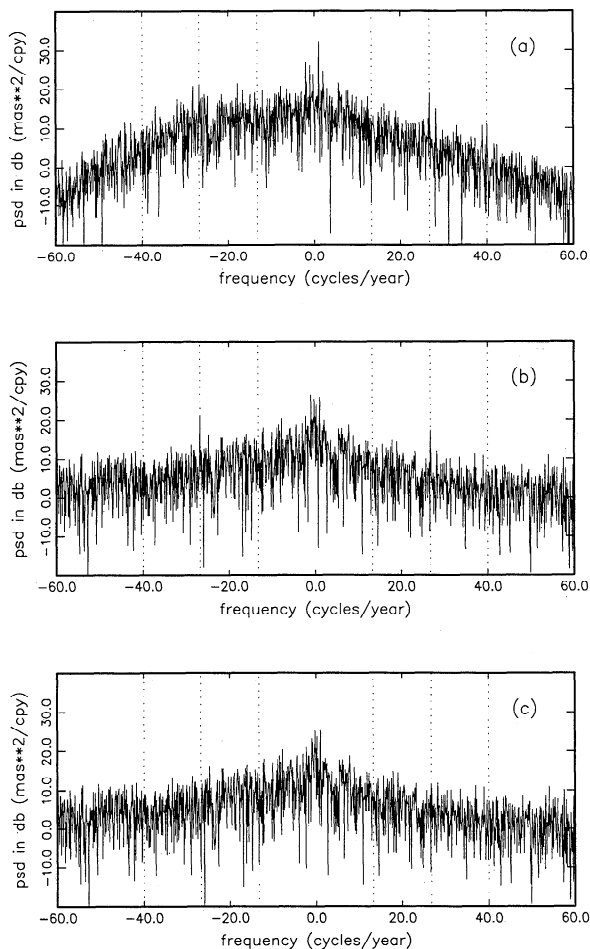


Figure 1. Power spectral density (psd) estimates (periodograms) in decibels (db) computed from time series of polar motion excitation functions $\chi(t)$ spanning 1984–1994 of: (a) the SPACE94 polar motion excitation function derived from space-geodetic Earth rotation measurements, (b) the residual polar motion excitation function formed by subtracting the AAM series from the SPACE94 excitation series, and (c) the result of removing the recovered tidal terms from the SPACE94–AAM residual series. The vertical dotted lines indicate frequencies in the prograde and retrograde weekly tidal bands (at ± 40.01 cpy), fortnightly tidal bands (at ± 26.74 cpy), and monthly tidal bands (at ± 13.26 cpy). The retrograde component of polar motion excitation is represented by negative frequencies, the prograde component by positive frequencies.

only the mean pressure over the world's oceans is transmitted to the underlying oceanic crust; or (2) the oceans are assumed to be "rigid", thereby fully transmitting the imposed atmospheric pressure variations to the ocean-bottom crust. At the periods of interest to this study (a week to a month) the oceans are generally believed to respond nearly as an inverted barometer [e.g., Dickman, 1988; Ponte *et al.*, 1991; Ponte, 1992, 1993, 1994] and hence this version of the pressure term was chosen for use here.

The AAM values used in this study are diagnostic variables computed from the output of an atmospheric general circulation model (GCM) operated for the primary purpose of forecasting the weather. Changes are often made to the GCM in order to improve the weather forecasts. These model changes also lead to improved AAM values, but have the undesired effect of sometimes causing sudden, step-like changes in the mean AAM

value, especially in the pressure term, at the time of the model change. These step-like changes in the mean value of the AAM pressure term have been removed here [D. Dong, personal communication, 1995] by applying a correction determined from the offset (at the time of the model change) of 2 smoothing splines, one fit to the values before the time of the model change, the second fit to the values after that time. In order to better estimate the amplitude of the step-like change, the smoothing splines were not fit to the NCEP AAM pressure term values themselves, but were instead fit to the values of a residual series formed by differencing the NCEP values with those determined independently by the Japan Meteorological Agency.

After correcting the AAM pressure term for the effects of model changes, missing values in the pressure and wind terms were filled by linear interpolation. Because of the diurnal and semidiurnal variations in atmospheric pressure and wind, and hence in the AAM pressure and wind terms, a missing AAM value was replaced by linearly interpolating between the nearest values on either side of the data gap that are given at the same hour (e.g., noon) as that of the missing value. In this manner, data gaps are filled by linear interpolation of values that are at the same phase in the diurnal and semidiurnal cycles as are the missing values.

After separately filling the gaps in the wind and pressure terms, the total atmospheric angular momentum values were formed by taking their sum. Daily averages of the total AAM values were then formed by averaging the twice-per-day values given from August 30, 1983 through June 20, 1992, and the four-times-per-day values given since June 21, 1992.

Figure 1b displays the power spectrum of the residual series formed by subtracting the AAM series from the SPACE94 polar motion excitation series during 1984–1994. Enhanced power is still evident in the prograde and retrograde fortnightly tidal bands, but is no longer evident in the prograde weekly tidal band (compare with Figure 1a).

Determination of an Empirical Model

In principle, ocean tidal sea level height and current changes at all tidal frequencies are capable of exciting polar motion, but in practice only the largest tides are likely to excite the polar motion to observable levels. In the weekly tidal band the largest ocean tides are the $M9'$ (9.12-day) and $M9$ (9.13-day) tides, in the fortnightly tidal band they are the Mf' (13.63-day) and Mf (13.66-day) tides, in the monthly band it is the Mm (27.55-day) tide, in the semiannual band it is the Ssa (182.62-day) tide, and in the annual band it is the Sa (365.26-day) tide. Of these tides, the amplitude of the tidal potential is greatest for Mf , followed, in order of decreasing amplitude, by Mm , Ssa , Mf' , $M9$, $M9'$, and is

Table 1. Expansion of the Tidal Argument

| Tide | Period (solar days) | Fundamental Argument | | | | |
|-------------|------------------------|----------------------|------|-----|-----|----------|
| | | l | l' | F | D | Ω |
| Weekly | | | | | | |
| $M9'$ | 9.12 | 1 | 0 | 2 | 0 | 1 |
| $M9$ | 9.13 | 1 | 0 | 2 | 0 | 2 |
| Fortnightly | | | | | | |
| Mf' | 13.63 | 0 | 0 | 2 | 0 | 1 |
| Mf | 13.66 | 0 | 0 | 2 | 0 | 2 |
| Monthly | | | | | | |
| Mm | 27.55 | 1 | 0 | 0 | 0 | 0 |
| Semiannual | | | | | | |
| Ssa | 182.62 | 0 | 0 | 2 | -2 | 2 |
| Annual | | | | | | |
| Sa | 365.26 | 0 | 1 | 0 | 0 | 0 |

Table 2. Observed and Predicted Effects of Long-Period Ocean Tides on the Polar Motion Excitation Function $\chi(t)$

| | Prograde | | Retrograde | |
|------------------------|-----------------|-----------------|-----------------|-----------------|
| | Amplitude (mas) | Phase (degrees) | Amplitude (mas) | Phase (degrees) |
| <i>M9'</i> (9.12-day) | | | | |
| SPACE94-AAM | 0.54 ± 0.45 | 38 ± 48 | 0.21 ± 0.45 | 79 ± 126 |
| Dickman | 0.13 | 73 | 0.21 | 15 |
| <i>M9</i> (9.13-day) | | | | |
| SPACE94-AAM | 0.47 ± 0.45 | -30 ± 55 | 0.41 ± 0.45 | -95 ± 63 |
| Dickman | 0.32 | 73 | 0.52 | 15 |
| <i>Mf'</i> (13.63-day) | | | | |
| SPACE94-AAM | 1.61 ± 0.45 | 56 ± 16 | 2.01 ± 0.45 | 87 ± 13 |
| Dickman | 0.52 | 100 | 0.71 | 8 |
| Seiler | 0.72 | 55 | 0.59 | 72 |
| <i>Mf</i> (13.66-day) | | | | |
| SPACE94-AAM | 0.86 ± 0.45 | 93 ± 30 | 2.73 ± 0.45 | 14 ± 10 |
| Dickman | 1.26 | 100 | 1.72 | 8 |
| Seiler | 1.72 | 55 | 1.44 | 72 |
| <i>Mm</i> (27.55-day) | | | | |
| SPACE94-AAM | 0.75 ± 0.45 | 49 ± 35 | 0.82 ± 0.45 | -59 ± 32 |
| Dickman | 0.47 | 136 | 0.28 | -7 |
| Seiler | 0.78 | 74 | 0.92 | 28 |

least for *Sa*. The small difference between the *Mf'* and *Mf* tidal frequencies, or between the *M9'* and *M9* tidal frequencies, corresponds to a beat period of 18.6 years. If polar motion excitation effects at these tidal frequencies are to be resolved, then a polar motion excitation time series spanning about 18.6 years must be analyzed. The entire SPACE94-AAM residual polar motion excitation series, spanning the 18.2 year-long interval of 1976.8–1994, was therefore used when fitting for periodic terms at these tidal frequencies.

Besides fitting for periodic terms at all the tidal frequencies listed in Table 1, the least-squares fit to the entire SPACE94-AAM residual polar motion excitation series also included terms for the mean and trend of the series. Table 2 gives the results and 1σ formal errors of the fit for the tidal terms in the weekly, fortnightly, and monthly tidal bands in terms of the amplitude A and phase α of the prograde and retrograde components of the polar motion excitation function defined by:

$$\chi(t) = A_p e^{i\alpha_p} e^{i\phi(t)} + A_r e^{i\alpha_r} e^{-i\phi(t)} \quad (2)$$

where the subscript p denotes prograde, the subscript r denotes retrograde, and $\phi(t)$ represents the tidal argument, the expansion of which is given in Table 1 for the individual terms being considered here. The results of the fit at the semiannual and annual tidal frequencies are not given in Table 2 since they include such unmodeled, nontidal polar motion excitation effects as seasonal changes in the general thermohaline circulation of the oceans. The results of the fit at the *Mf'* and *Mf* tidal frequencies have been resolved, as have those at the *M9'* and *M9* tidal frequencies, as evidenced by examining the covariance matrix of the fit, which shows the largest correlation coefficient between the solved-for periodic parameters to be 0.024.

Figure 1c displays the power spectrum of the series obtained by removing the fitted terms from the SPACE94-AAM residual series spanning 1984–1994. As can be seen, there is no longer any evidence of enhanced power in the prograde or retrograde fortnightly tidal bands. Thus, the empirical fortnightly tide model given in Table 2 (obtained upon fitting the full series spanning 1976.8–1994) can fully account for the enhanced power in the fortnightly tidal band evident in the SPACE94-AAM residual polar motion excitation series, either in the full series (not shown but also not surprising since the least-squares fit is to the full series), or in that subset spanning 1984–1994 (Figure 1).

Comparison to Predictions of Ocean Tide Models

Seiler [1991], using a hydrodynamic ocean tide model, computed the axial and both equatorial components of the angular momentum associated with tidal changes in sea level height and currents for three semidiurnal (M_2 , S_2 , N_2), three diurnal (K_1 , O_1 , P_1), and four long-period tides (Mf' , Mf , Mm , Ssa). The effects of the four long-period ocean tides (the sum of the sea level height and current terms) on the polar motion excitation function $\chi(t)$ predicted from Seiler's ocean tidal angular momentum results are given in Table 2 in terms of the amplitude and phase of the prograde and retrograde components.

Dickman [1993] developed broadband Liouville equations and used them to predict the Earth rotation effects of 32 short- and long-period ocean tides using tide heights and currents computed from his spherical harmonic ocean tide model. The effects of long-period ocean tides (the sum of the sea level height and current terms) on the polar motion excitation function $\chi(t)$ predicted by Dickman's ocean tide model are computed here using equation (1) and the tabulated polar motion results of Dickman [1993, Table 3f], and are given in Table 2 in terms of the amplitude and phase of the prograde and retrograde components. (Note that in Dickman [1993] the tabulated ocean tidal effects on the prograde and retrograde components of polar motion were inadvertently switched [S. R. Dickman, personal communication, 1995]. In computing here the predicted effect on the polar motion excitation function, the tabulated prograde polar motion component of Dickman [1993, Table 3f] has been interpreted to be, in fact, the retrograde component, and vice versa).

At the *Mf* and *Mf'* tidal frequencies, the Dickman and Seiler predicted amplitudes agree reasonably well with each other, with the prograde amplitudes predicted by Dickman's model being 27 percent smaller than those predicted by Seiler's model, and the retrograde amplitudes being 19 percent larger. However, the predicted phases differ by 45° for the prograde components, and 64° for the retrograde components. At the *Mm* tidal frequency, the amplitude of the polar motion excitation function predicted by Dickman's model is substantially smaller than that predicted by Seiler's model, being 0.47 mas for the prograde component (versus 0.78 mas for that predicted by Seiler's model) and 0.28 mas for the retrograde component (versus 0.92 mas for that predicted by Seiler's model). The predicted phases again show large discrepancies of 62° for the prograde component and 35° for the retrograde component. Of the long-period ocean tides considered, the smallest polar motion excitation effects are predicted by Dickman's ocean tide model to occur at the *M9'* tidal frequency, being 0.13 mas and 0.21 mas for the amplitudes of the prograde and retrograde components, respectively.

At the *Mf* tidal frequency, the observations agree best with the predictions of Dickman's model, with the predicted amplitudes being 47 percent larger for the prograde component and 37 percent smaller for the retrograde component than those observed, but with the phases differing by only 7° for the prograde component and 6° for the retrograde component. The agreement of the observations with the predictions of Seiler's model is substantially worse at the *Mf* tidal frequency than it is with the predictions of Dickman's model, with both prograde and retrograde amplitudes differing from the observations by about a factor of 2, and the prograde and retrograde phases differing by 38° and 58° , respectively.

However, at the *Mf'* tidal frequency, the observations agree better, at least in phase, with the predictions of Seiler's model than they do with the predictions of Dickman's model. The Seiler model's predicted prograde and retrograde phases differ from the observations by only 1° and 15° , respectively, although the predicted amplitudes for the prograde component are less than one-half that observed, and for the retrograde component it is less than one-third that observed. Dickman's model predictions at the *Mf'* tidal frequency show greater disagreement with the observations than do Seiler's model predictions, with phases

differing by 44° and 79° for the prograde and retrograde components, respectively, the prograde amplitude being less than one-third that observed, and the retrograde amplitude being a bit more than one-third that observed.

The observed results at the $M9'$ and $M9$ tidal frequencies are at the level of the formal uncertainty, and Figure 1b shows no evidence of enhanced power in either the prograde or retrograde weekly tidal bands, so there is no detectable evidence for polar motion excitation by these ocean tides. At the Mm tidal frequency, the observed effect is somewhat larger than the formal uncertainty, but Figure 1b again shows no evidence of enhanced power in either the prograde or retrograde monthly tidal bands. This indicates that the formal uncertainties given in Table 2 may have been underestimated, and inflating them by about a factor of two may give more realistic estimates of the uncertainties.

Discussion

There have been at least 3 other recent investigations into long-period ocean tidal excitation of polar motion. Schuh [1990] found a 13.7-day signal in the crosstrack component of polar motion $\mathbf{p}(t)$ having an amplitude of 1.0 mas and a phase consistent with that expected from forcing by the Mf ocean tide. From equation (1), a polar motion excitation amplitude of about 32 mas is required to force a periodic polar motion signal of 1.0 mas amplitude at the Mf tidal frequency, a forcing amplitude that is an order of magnitude larger than that found here (Table 2). Chao [1994; personal communication, 1996] found evidence for both a 9-day signal in polar motion excitation $\chi(t)$, as well as polar motion excitation signals having x and y component amplitudes of 1.2 mas and 4.7 mas, respectively, at the Mf tidal frequency, and 1.9 mas and 1.8 mas, respectively, at the Mf' tidal frequency. These fortnightly polar motion excitation amplitudes are of the same order of magnitude as those found here (Table 2). Dickman and Nam [1995] determined fortnightly prograde and retrograde polar motion $\mathbf{p}(t)$ amplitudes of 0.061 ± 0.079 mas and 0.063 ± 0.063 mas, respectively. From equation (1), a polar motion excitation amplitude of about 2 mas is required to force a periodic polar motion signal of 0.06 mas amplitude at the Mf tidal frequency, a polar motion excitation amplitude that is again of the same order of magnitude as that found here (Table 2).

Predictions from the two available ocean tide models for the effect of the fortnightly ocean tides on the polar motion excitation function $\chi(t)$ agree reasonably well with each other in amplitude (although not in phase). However, except for the prograde Mf tidal signal, the predicted amplitudes are considerably smaller than those observed. This indicates that either: (1) both tide models have systematically underestimated the polar motion effect, (2) there are other geophysical mechanisms contributing to the observed effect, or (3) the observed residual polar motion excitation series is contaminated by either measurement noise or errors at the fortnightly tidal frequencies. It is certainly possible, and even probable, that errors exist in both the space-geodetic measurements and the AAM series, especially prior to 1984, although it is difficult to understand why they would be more prominent at the fortnightly tidal frequencies rather than having a more broadband character.

Evidence for either noise contamination or the presence of other geophysical mechanisms also comes from an examination of the recovered prograde and retrograde phases of the Mf' and Mf tidal signals. If ocean tides were the only cause of the observed fortnightly signals, then the phase of the prograde Mf' and Mf signals should agree with each other, as should the phases of the retrograde signals [S. R. Dickman, personal communication, 1995]. From Table 2, the phases of the prograde Mf' and Mf signals agree with each other to within about 1σ , but

the retrograde phases do not. One possible additional contributor to the observed fortnightly tidal polar motion excitation signal could be tidal polar motion excitation changes caused by lateral inhomogeneities in the density structure of the crust and mantle, although a quantitative evaluation of this effect must await further investigation.

Acknowledgments. One of us (RSG) gratefully acknowledges the assistance given by S. Dickman in helping to understand the predicted Earth rotation effects of his ocean tide model. The work described in this paper was performed at the Jet Propulsion Laboratory, California Institute of Technology, under contract with the National Aeronautics and Space Administration.

References

- Chao, B. F., Zonal tidal signals in the Earth's polar motion (abstract), *Eos Trans. AGU*, 75(44), Fall Meeting Suppl., 158, 1994.
- Dickman, S. R., Theoretical investigation of the oceanic inverted barometer response, *J. Geophys. Res.*, 93, 14941–14946, 1988.
- Dickman, S. R., Dynamic ocean-tide effects on Earth's rotation, *Geophys. J. Int.*, 112, 448–470, 1993.
- Dickman, S. R., and Y. S. Nam, Revised predictions of long-period ocean tidal effects on Earth's rotation rate, *J. Geophys. Res.*, 100, 8233–8243, 1995.
- Eubanks, T. M., Variations in the orientation of the Earth, in *Contributions of Space Geodesy to Geodynamics: Earth Dynamics*, Geodyn. Ser., vol. 24, edited by D. E. Smith and D. L. Turcotte, pp. 1–54, AGU, Washington, D.C., 1993.
- Gross, R. S., Correspondence between theory and observations of polar motion, *Geophys. J. Int.*, 109, 162–170, 1992.
- Gross, R. S., Combinations of Earth orientation measurements: SPACE94, COMB94, and POLE94, *J. Geophys. Res.*, in press, 1996.
- Herring, T. A., Diurnal and semidiurnal variations in Earth rotation, in *Observations of Earth From Space*, edited by R. P. Singh, M. Feissel, B. D. Tapley, and C. K. Shum, *Adv. Space Res.*, 13(11), 281–290, 1993.
- Herring, T. A., and D. Dong, Measurement of diurnal and semidiurnal rotational variations and tidal parameters of Earth, *J. Geophys. Res.*, 99, 18051–18071, 1994.
- Morabito, D. D., T. M. Eubanks, and J. A. Steppe, Kalman filtering of Earth orientation changes, in *The Earth's Rotation and Reference Frames for Geodesy and Geodynamics*, edited by A. K. Babcock and G. A. Wilkins, pp. 257–267, D. Reidel, Norwell, Mass., 1988.
- Ponte, R. M., The sea level response of a stratified ocean to barometric pressure forcing, *J. Phys. Oceanogr.*, 22, 109–113, 1992.
- Ponte, R. M., Variability in a homogenous global ocean forced by barometric pressure, *Dyn. Atmos. Oceans*, 18, 209–234, 1993.
- Ponte, R. M., Understanding the relation between wind- and pressure-driven sea level variability, *J. Geophys. Res.*, 99, 8033–8039, 1994.
- Ponte, R. M., D. A. Salstein, and R. D. Rosen, Sea level response to pressure forcing in a barotropic numerical model, *J. Phys. Oceanogr.*, 21, 1043–1057, 1991.
- Schuh, H., Earth's rotation measured by VLBI, in *Earth's Rotation from Eons to Days*, edited by P. Brosche and J. Sündermann, pp. 1–12, Springer-Verlag, Berlin, 1990.
- Seiler, U., Periodic changes of the angular momentum budget due to the tides of the world ocean, *J. Geophys. Res.*, 96, 10287–10300, 1991.
- Sovers, O. J., C. S. Jacobs, and R. S. Gross, Measuring rapid ocean tidal Earth orientation variations with VLBI, *J. Geophys. Res.*, 98, 19959–19971, 1993.
- Watkins, M. M., and R. J. Eanes, Diurnal and semidiurnal variations in Earth orientation determined from LAGEOS laser ranging, *J. Geophys. Res.*, 99, 18073–18079, 1994.
- Yoder, C. F., J. G. Williams, and M. E. Parke, Tidal variations of Earth rotation, *J. Geophys. Res.*, 86, 881–891, 1981.

D. H. Boggs, R. S. Gross and K. H. Hamdan, Jet Propulsion Laboratory, Mail Stop 238-332, 4800 Oak Grove Drive, Pasadena, CA 91109-8099 (e-mail: rsg@logos.jpl.nasa.gov)

(Received November 6, 1995; revised February 5 1996; accepted March 11, 1996)